

NASA TM X-677

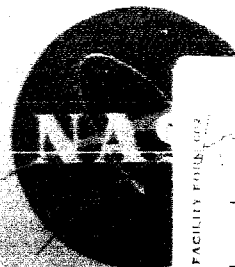
GPO PRICE

CFSTI PRICE

Hard copy price

Microfilm price

1965-1 July 66



FACILITY FOR 102

N66 33345

ARTICLE DELIVERED

29
(PAGES)

TMX-677

(NASA OR OR TMX OR AD NUMBER)

(CODE)

31
(CATEGORY)

NASA TM X-677

TECHNICAL MEMORANDUM

X-677

PRELIMINARY INVESTIGATION OF INTERFERENCE EFFECTS OF MULTICOPLANAR FINS ON A TWO-STAGE ROCKET LAUNCH VEHICLE WITH WINGED SPACECRAFT AT TRANSONIC SPEEDS

By P. Kenneth Pierpont

Langley Research Center
Langley Station, Hampton, Va.

DECLASSIFIED- AUTHORITY
US: 1286 DROBKA TO LEBOW
MEMO DATED
6/8/66

Declassified by authority of NASA
Classification Change Notices No 67
Dated ** 6/29/66

NATIONAL AERONAUTICS AND SPACE ADMINISTRATION
WASHINGTON

April 1962

DECLASSIFIED

NATIONAL AERONAUTICS AND SPACE ADMINISTRATION

TECHNICAL MEMORANDUM X-677

PRELIMINARY INVESTIGATION OF INTERFERENCE EFFECTS
OF MULTICOPLANAR FINS ON A TWO-STAGE ROCKET LAUNCH VEHICLE
WITH WINGED SPACECRAFT AT TRANSONIC SPEEDS*

By P. Kenneth Pierpont

SUMMARY

33345

A preliminary investigation has been made in the Langley 8-foot transonic pressure tunnel to determine the transonic aerodynamic characteristics of a two-stage fin-stabilized rocket launch vehicle in combination with a winged spacecraft. Effects of the winged spacecraft on the stability and axial-force contributions of the second-stage fins have been determined. The investigation was made for a range of test Mach numbers from 0.60 to 1.20 and a range of angles of attack from about -2° to 10° at 0° sideslip. Reynolds number for the tests varied from 3.2×10^6 to 4.2×10^6 per foot.

Installation of the first-stage fins reduced the variation of longitudinal stability parameter with Mach number to a negligible amount. The interference of the winged spacecraft decreased the magnitude of the stability contribution of the second-stage fins by about one-half and resulted in a negligible axial-force-coefficient penalty attributable to the second-stage fins.

INTRODUCTION

The addition of winged spacecraft, which may be required for manned reentry vehicles having airplane-like landing characteristics, to multistage-rocket configurations can be expected to introduce serious stability problems in the transonic region. Such spacecraft may require the use of stabilizing fins on one or more of the lower stages of a multistage launch vehicle. Therefore, a preliminary investigation has been made to obtain transonic stability characteristics and interference effects of a two-stage rocket launch vehicle having a winged spacecraft and multicoplanar stabilizing fins.

*Title, Unclassified.

031717201030

An existing research model was modified to incorporate first- and second-stage fins to be tested in conjunction with a winged spacecraft. Various arrangements of the spacecraft wing and launch-vehicle fins were tested to determine the basic stability of the configuration and some of the interference effects when the fins and/or wings were coplanar. Three-component force and moment data were obtained in the Langley 8-foot transonic pressure tunnel at Mach numbers from 0.60 to 1.20 and for an angle-of-attack range from about -2° to 10° . Reynolds number for the tests varied from about 3.2×10^6 to 4.2×10^6 per foot.

SYMBOLS

C_N	normal-force coefficient, $\frac{\text{Normal force}}{qA}$
C_A	axial-force coefficient, $\frac{\text{Axial force}}{qA}$
$C_{A,b}$	base axial-force coefficient
$C_{A,o}$	axial-force coefficient at $\alpha = 0^\circ$
C_m	pitching-moment coefficient (referred to model base), $\frac{\text{Pitching moment}}{qAD}$
C_{mC_N}	longitudinal stability parameter, $\partial C_m / \partial C_N$
$C_{N\alpha}$	normal-force-curve slope, $\partial C_N / \partial \alpha$
ΔC_{mC_N}	increment in longitudinal stability parameter at $\alpha = 0^\circ$
$\Delta C_{A,o}$	increment in axial-force coefficient at $\alpha = 0^\circ$
A	maximum model frontal area, $\frac{\pi D^2}{4}$, sq ft
c	local chord, in.

D	maximum body diameter, ft
M	free-stream Mach number
q	free-stream dynamic pressure, lb/sq ft
R	Reynolds number per foot
S	exposed wing surface area, sq ft
$x_{c.p.}/D$	nondimensional center-of-pressure location, measured from model base
α	angle of attack, deg
β	angle of sideslip, deg

MODEL DESCRIPTION

The basic model consisted of a two-stage rocket launch vehicle plus a spacecraft. (See fig. 1(a).) Fineness ratio for the launch vehicle was approximately 9.5. Stabilizing fins were provided for both stages of the vehicle (fig. 1(b)). These fins were of simple delta planform with approximately 70° leading-edge sweepback and had thickness ratios of 0.02 and 0.05 for the first and second stages, respectively. The spacecraft wing was also of delta planform with 70° leading-edge sweepback. The thickness ratio of this surface was 0.10. The stabilizing fins and spacecraft wing were mounted at 0° incidence and were coplanar. Table I summarizes the geometric characteristics of the model.

APPARATUS AND TESTS

The tests were made in the Langley 8-foot transonic pressure tunnel over a Mach number range from 0.60 to 1.20 and an angle-of-attack range from about -2° to about 10° at 0° sideslip. Transition was fixed on the nose of the spacecraft and at the 10-percent-chord station on all aerodynamic surfaces. Three-component force and moment data were obtained by use of an internally mounted strain-gage balance. Force coefficients were referred to the maximum cross-sectional area of the first rocket stage and the pitching-moment coefficient was taken about the model base. (See fig. 1(a).) The variation of test Reynolds number per foot with Mach number is shown in figure 2; the Reynolds number per foot varied from about 3.2×10^6 to 4.2×10^6 .

03:10:00:1030

The angle of attack was corrected for sting and balance deflections under load. Base pressures were measured and the axial-force coefficient was adjusted to correspond to a base pressure equal to the free-stream value. Representative variations of base axial-force coefficient with angle of attack at several Mach numbers are shown in figure 3.

Estimated accuracy of the data, based on balance accuracy and repeatability, is shown as follows:

M	±0.005	
α , deg	±0.1	L
C_N	±0.05	1
C_A	±0.01	8
C_m	±0.2	9
		1

PRESENTATION OF RESULTS

The results of this investigation have been reduced to standard NASA coefficients referred to the body axes, and parameter forms are presented in the following figures:

	Figure
Base axial-force coefficient as a function of angle of attack for the basic configuration without and with first-stage fins; $\beta = 0^\circ$	3
Aerodynamic characteristics of the basic configuration without and with first-stage fins; $\beta = 0^\circ$	4
Effect of addition of second-stage fins and winged spacecraft on the aerodynamic characteristics of the finned launch vehicle; $\beta = 0^\circ$	5
Effect of removal of the second-stage fins on the aerodynamic characteristics of the model with winged spacecraft; $\beta = 0^\circ$	6
Comparison of the variation with Mach number of the axial-force coefficient and longitudinal stability parameters for the several configurations; $\alpha = 0^\circ$	7
Interference effects of the several fin-body arrangements on the aerodynamic characteristics	8
Comparison of the center-of-pressure location for the several model configurations	9

DISCUSSION OF RESULTS

Figures 4, 5, and 6 indicate that all of the configurations exhibited small nonlinear variations of C_N and C_m with angle of attack; however, no discontinuities in the curves are indicated. The variations in longitudinal stability with angle of attack are not considered severe for this type of configuration and, hence, would not require excessive control forces, whether obtained by aerodynamic control or engine gimbaling.

The addition of the first-stage fins is shown in figure 7 to have reduced the longitudinal stability parameter by a factor of 3 at 0° angle of attack. More importantly, the magnitude of the change in the longitudinal stability parameter with Mach number, which varied from 9.2 to 12 for the model with no fins, is shown to have been reduced by the addition of the first-stage fins to only 2.3 to 2.7, which is considered a negligible variation. The change in magnitude of the stability parameter of figure 7 is shown in figure 8 as ΔC_{mC_N} , where ΔC_{mC_N} is obtained by taking the difference in C_{mC_N} of the immediately preceding configuration and the configuration in question. Thus, the curve labeled "First-stage fins" in figure 8 represents the change in C_{mC_N} with the fins-on from that for the fins-off configuration. A measure of the interference of the winged spacecraft on the effectiveness of the second-stage fins can be seen in this figure. When the second-stage fins were added to the configuration with first-stage fins, ΔC_{mC_N} is shown to vary between 1.4 and 1.9. However, when the second-stage fins were removed from the configuration which had all three sets of fins, ΔC_{mC_N} varied only between about -0.5 and -0.8. It may be concluded therefore that the contribution to the stability parameter due to the second-stage fins has been decreased in magnitude by more than one-half as a result of the interference of the winged spacecraft.

The improvement in stability resulting from the addition of the first-stage fins is further demonstrated in figure 9, in which the variation of the center-of-pressure location with angle of attack has been reduced to a negligible amount. With no fins, the center of pressure varied from 9.3 to 12.2 calibers from the base; whereas, with the first-stage fins installed it was moved rearward and varied only between 2.2 and 2.8 calibers from the base.

A comparison of the variation of the axial-force coefficient with Mach number for the various fin arrangements is shown in figure 7(a).

03: 4: 10: 30

Figure 8(a) shows the change in the axial-force coefficient $\Delta C_{A,0}$ for each configuration relative to the immediately preceding configuration. The data show that, when the first-stage fins were added, the axial-force coefficient increased between 0.062 and 0.122 at $M = 0.6$ and $M = 1.2$, respectively. When the second-stage fins were added, an additional axial-force-coefficient increment of from 0.042 to 0.069 is shown. When, however, the third-stage fins were added, $\Delta C_{A,0}$ was first positive at $M = 0.6$ and equal to about 0.07 but decreased rapidly through the transonic region to about -0.02 at $M = 1.2$. Although the accuracy of the data is probably no better than ± 0.01 , it appears that, at the worst, the configuration with all three sets of fins attached possessed no larger axial force than that with only the first- and second-stage fins. The streamwise cross section of the third-stage wing had a constant thickness which was 10 percent of the local wing chord with a semicircular leading-edge radius of 0.05 of the local chord. A wing of this design will, at transonic speeds, produce a strong bow wave accompanied by reduced dynamic pressure and Mach number in its wake. The second-stage fins and portions of the first-stage fins, operating in this wake, would not be expected to produce as large a wave drag as would be expected if they were exposed to the free-stream conditions. If this assumption is correct, this phenomenon may account for the negligible change in axial-force coefficient shown in figure 8(a) for the configuration with the second-stage fins removed and only the first-stage and spacecraft fins on. This type of interference would also account for the decrease in second-stage stability contribution discussed previously. It is recommended that further studies of this phenomenon be made which would include, in addition to force measurements, measurements of both static and total pressures in the vicinity of the first- and second-stage stabilizing fins.

SUMMARY OF RESULTS

A preliminary investigation to determine the transonic aerodynamic effects of a winged spacecraft and multicoplanar fins on a two-stage rocket launch vehicle has been made in the Langley 8-foot transonic pressure tunnel. The test Mach number was varied from 0.6 to 1.20 and the angle of attack from -2° to 10° . Corresponding test Reynolds number per foot varied from 3.2×10^6 to 4.2×10^6 . The principal results are as follows:

1. The installation of first-stage fins on the basic launch vehicle reduced the magnitude of the longitudinal stability parameter by a factor of 3 at 0° angle of attack and reduced the variation with Mach number to a negligible amount.

DECLASSIFIED

7

2. Interference of the winged spacecraft decreased the contribution of the second-stage fins to the longitudinal stability parameter by about one-half and decreased the corresponding increment in axial-force coefficient to a negligible amount.

Langley Research Center,
National Aeronautics and Space Administration,
Langley Air Force Base, Va., January 31, 1962.

1
1
3
2
1

[REDACTED]

09/12/88 1038

TABLE I.- GEOMETRIC CHARACTERISTICS OF MODEL

Rocket launch vehicle:

Length overall, in.	32.10
Maximum diameter, in.	2.52
Stage diameter ratio	0.95
Maximum cross-sectional area, sq in.	4.99
Length-diameter ratio	12.75
Moment reference center, in. from base	0.00

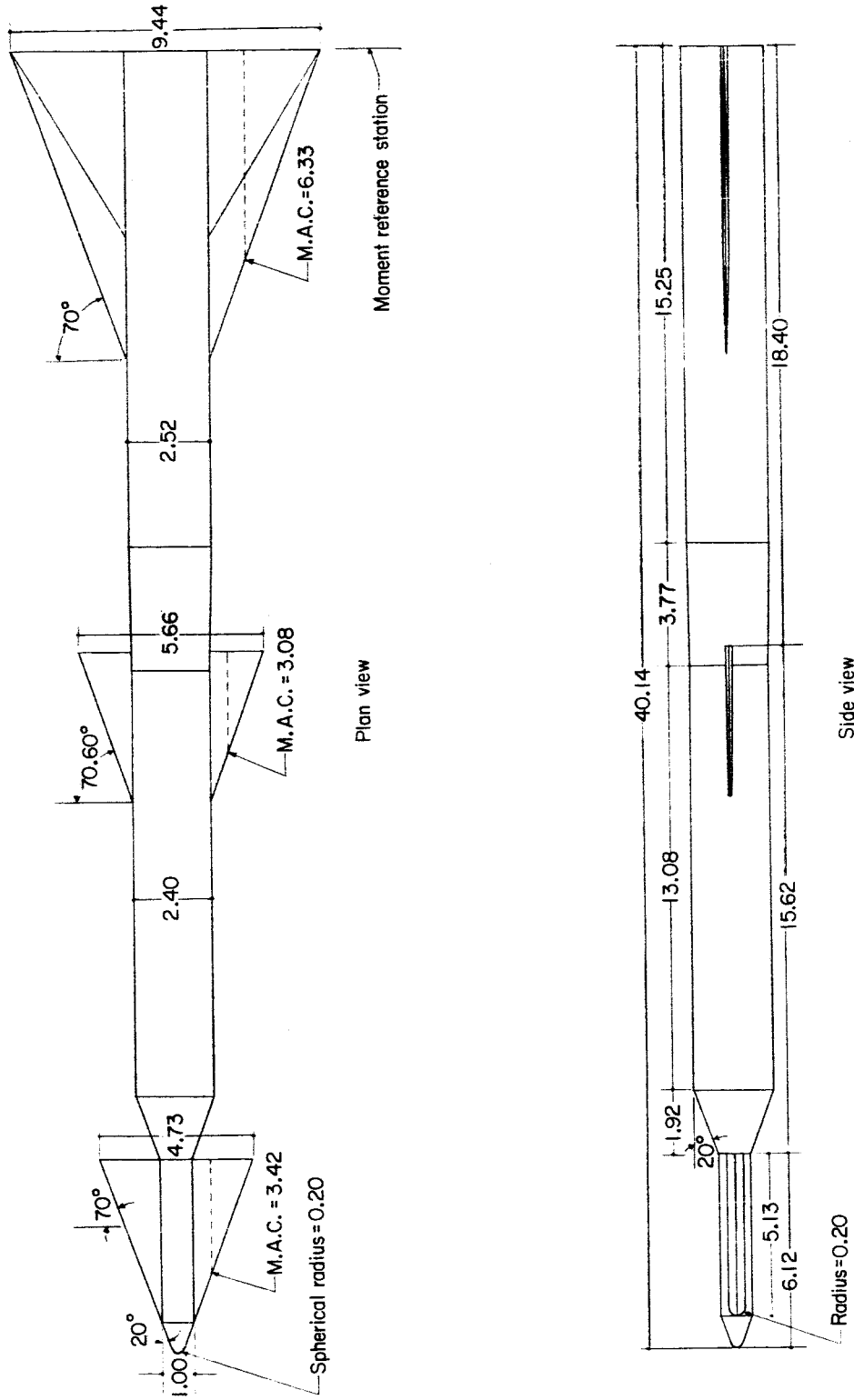
Spacecraft:

Length overall, in.	8.04
Diameter, in.	1.00

Aerodynamic surfaces:

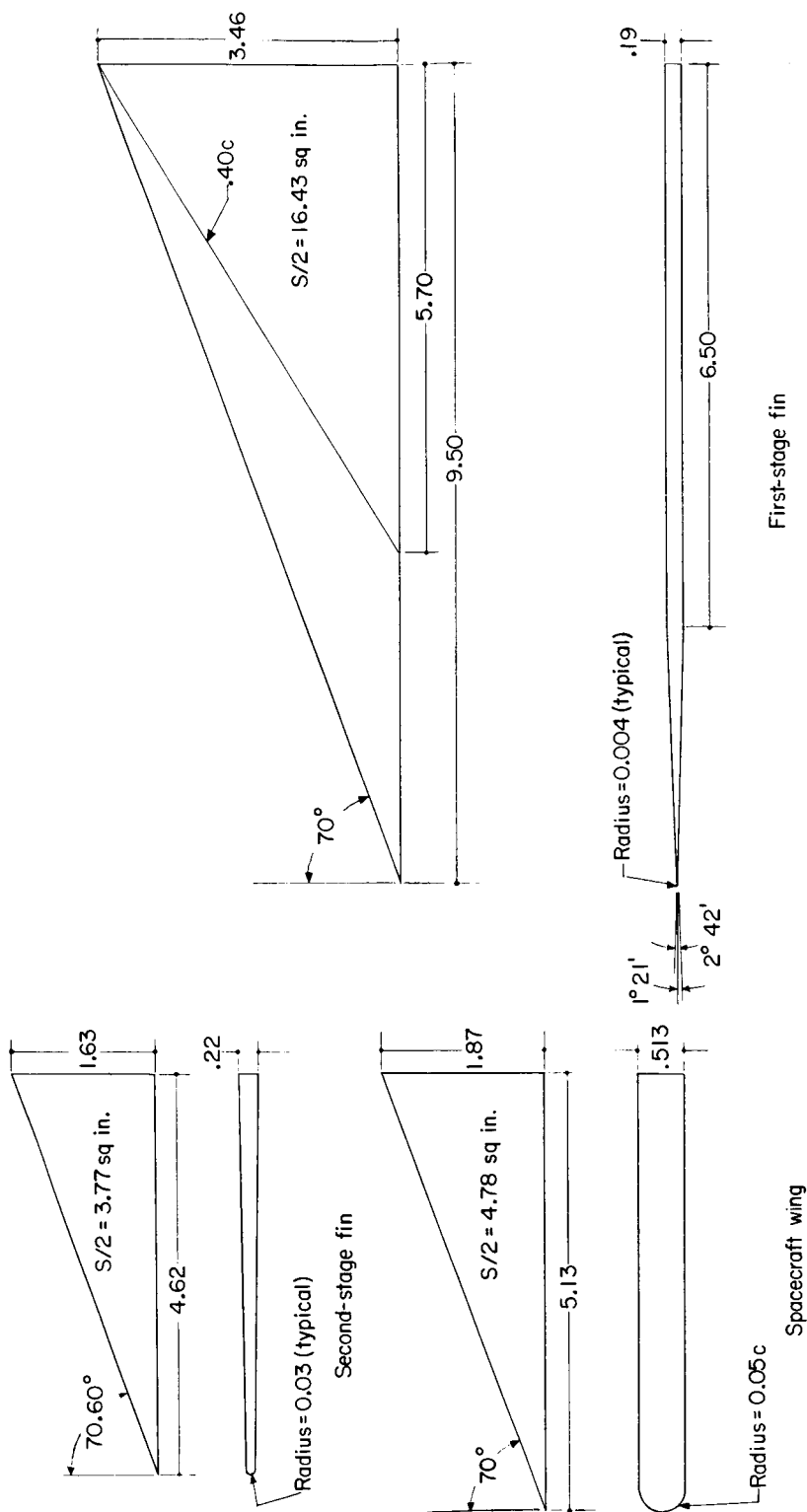
	Stage I	Stage II	Stage III
Total exposed area, sq in.	32.86	7.54	9.56
Total span, in.	9.44	5.66	4.73
Root chord, in.	9.50	4.62	5.13
Leading-edge sweep angle, deg	70	70.60	70
Thickness ratio	0.02	0.05	0.10
Leading-edge radius	0.004 in.	0.03 in.	0.05c

L
1
8
9
1



(a) General arrangement of complete model.

Figure 1.- Model details. All linear dimensions are in inches.



(b) Details of fins and spacecraft wing.

Figure 1.- Concluded.

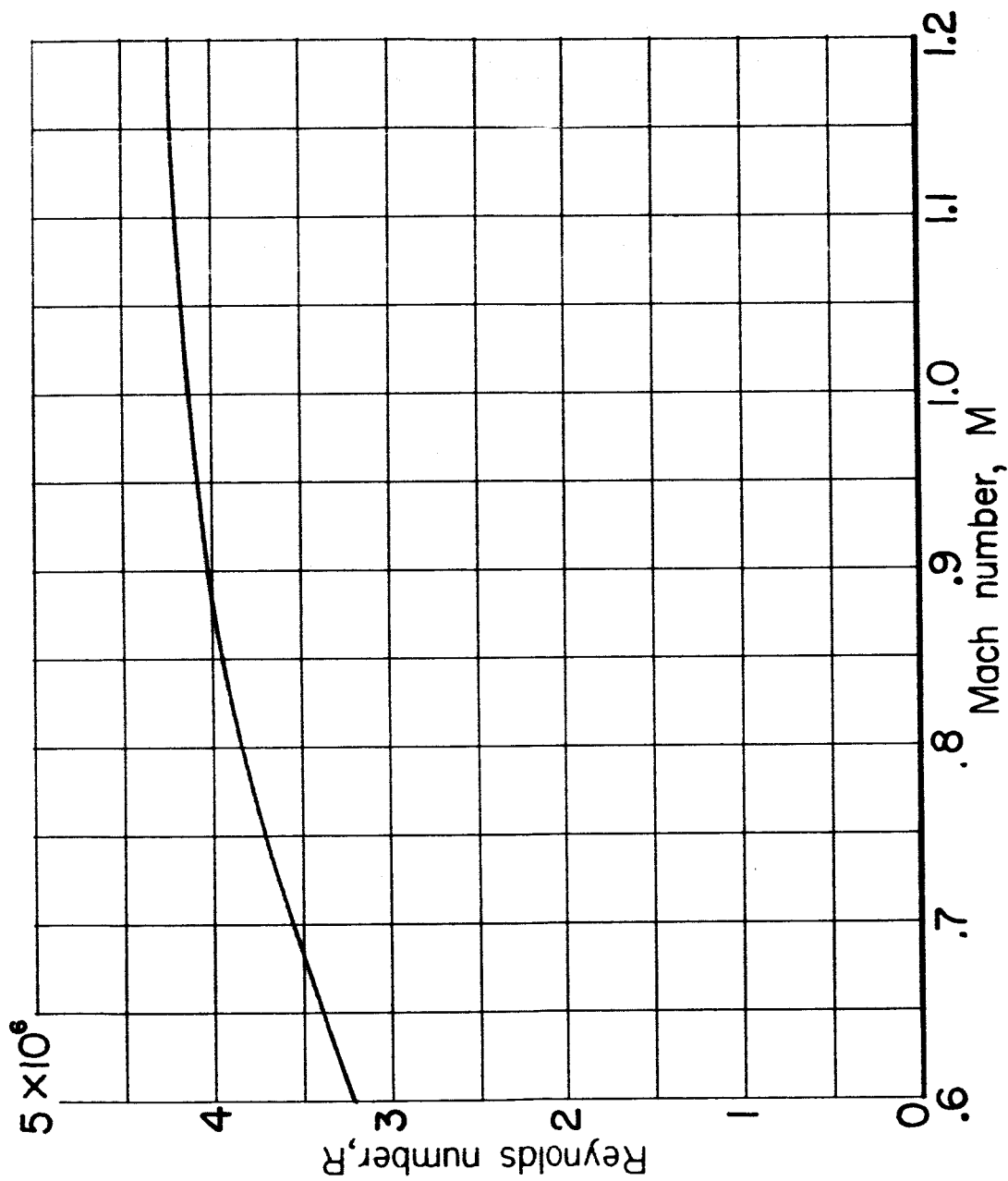


Figure 2.- Variation with Mach number of test Reynolds number per foot.

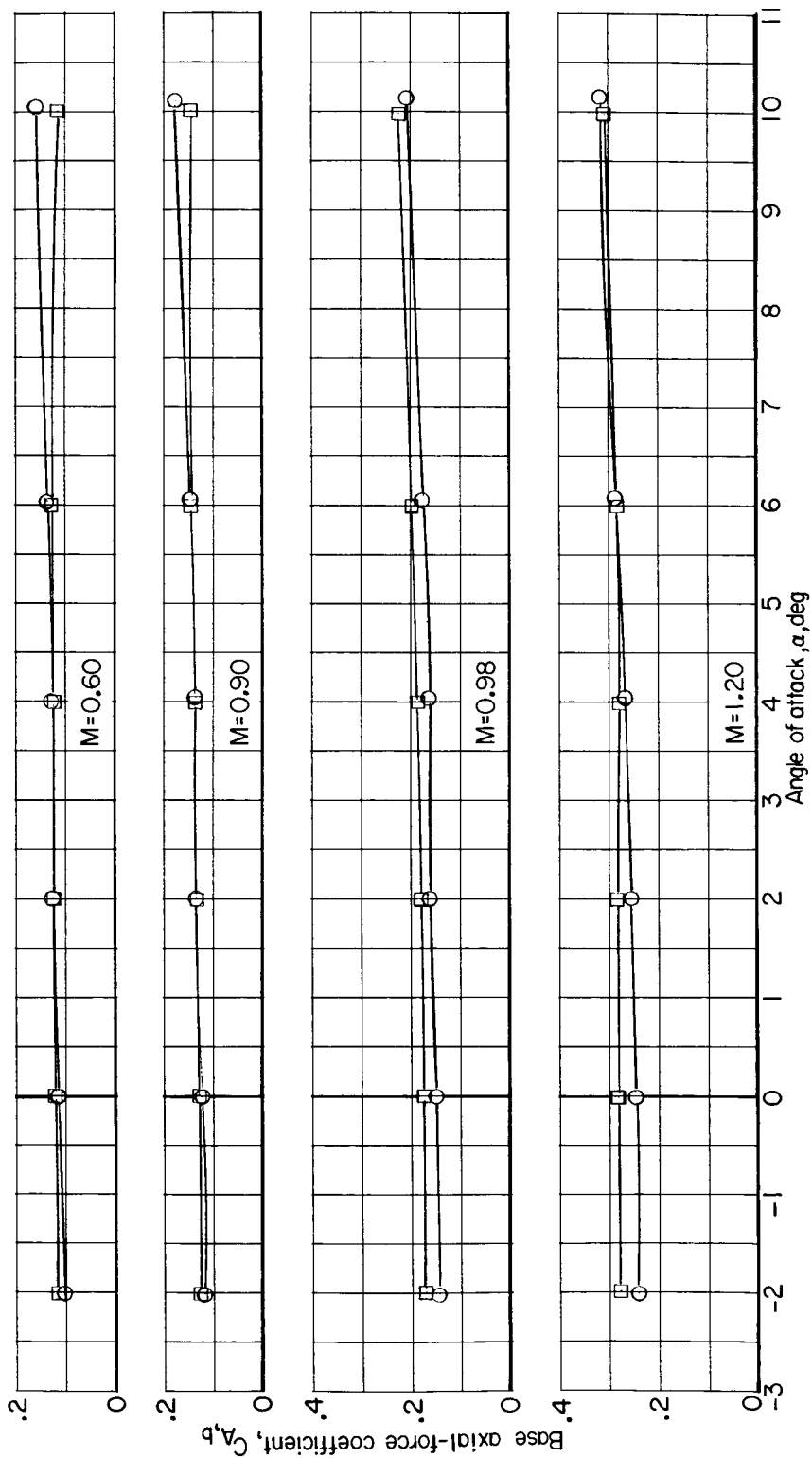
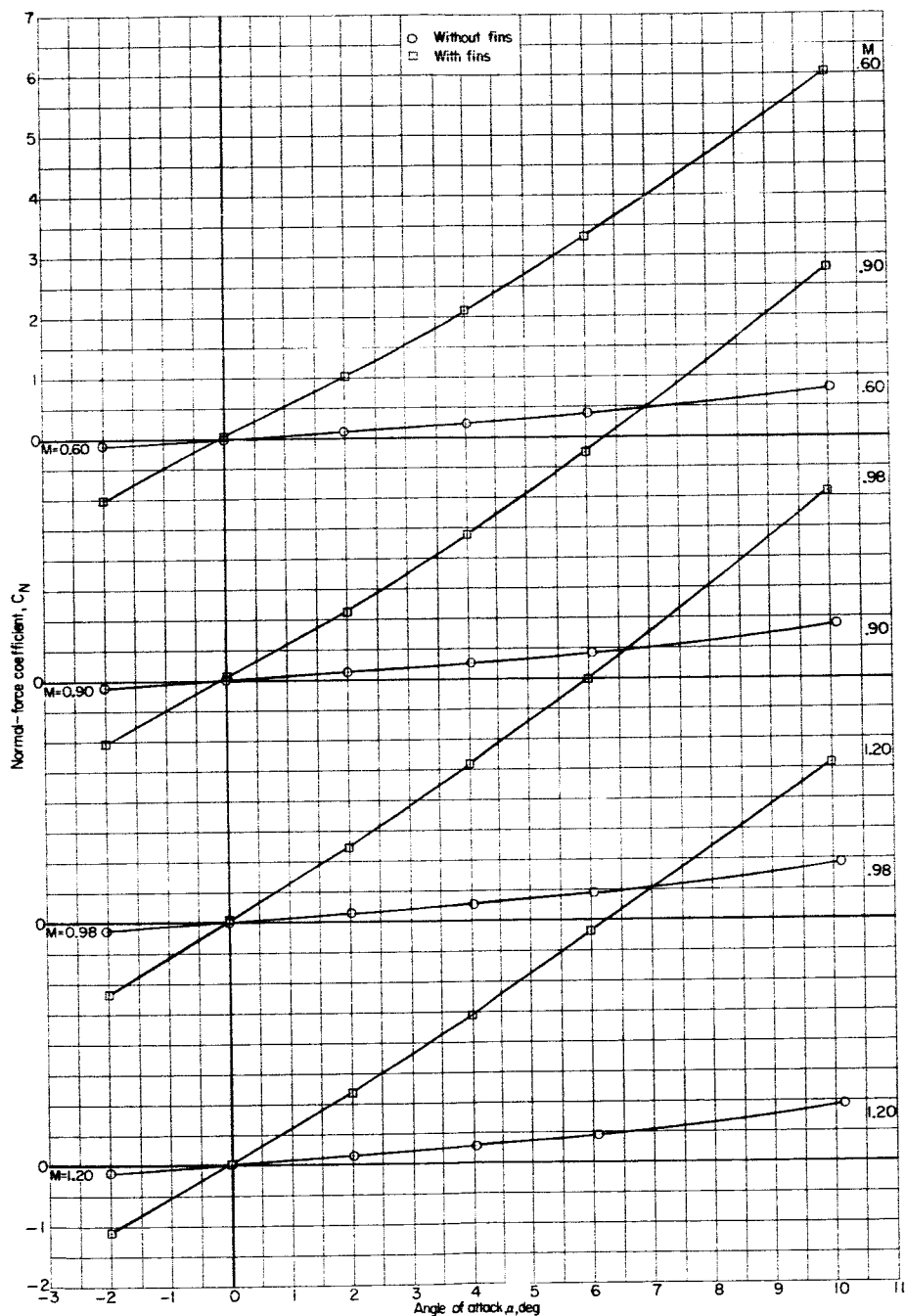


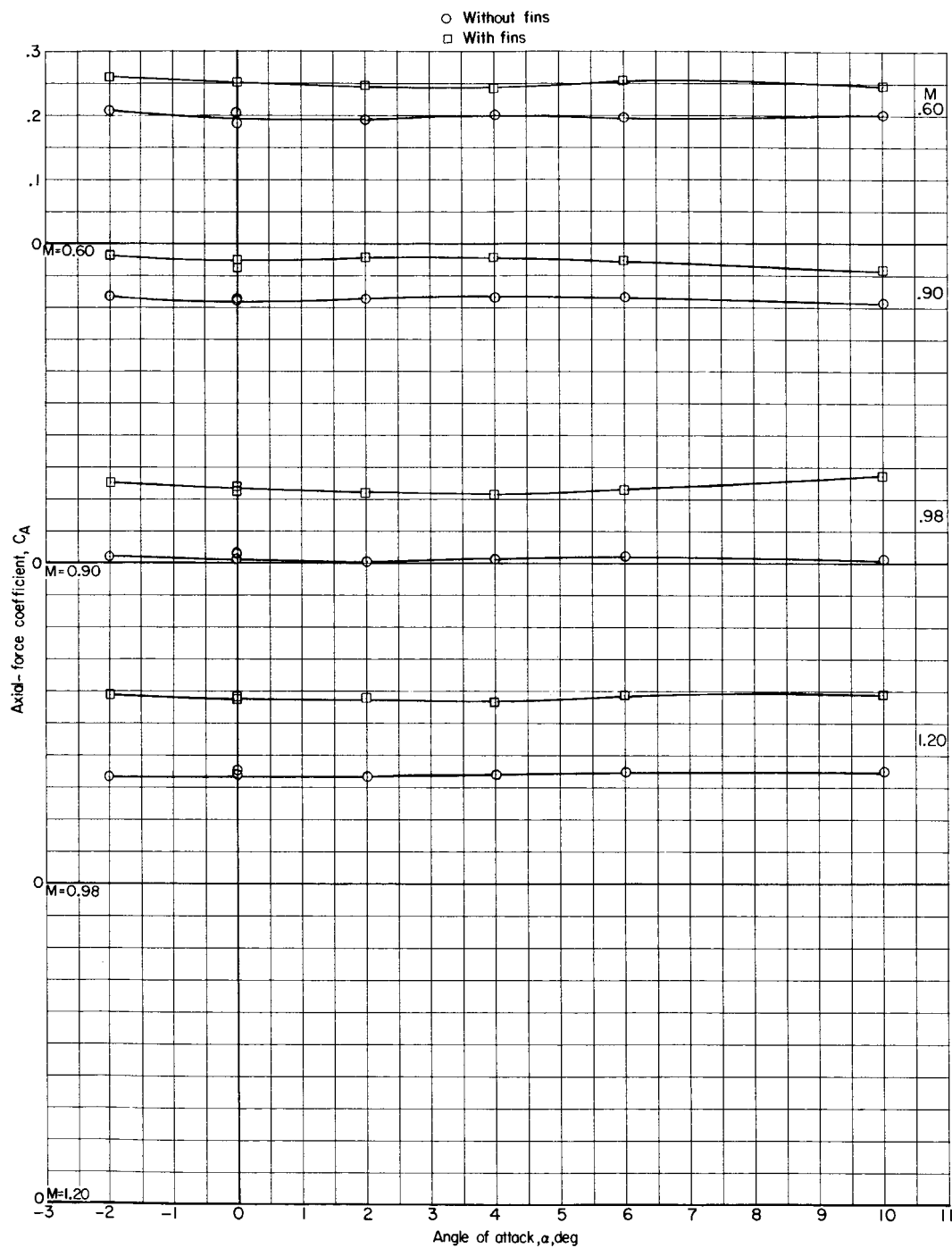
Figure 3.- Base axial-force coefficient against angle of attack for the basic configuration without and with first-stage fins. $\beta = 0^\circ$.



(a) Normal-force coefficient against angle of attack.

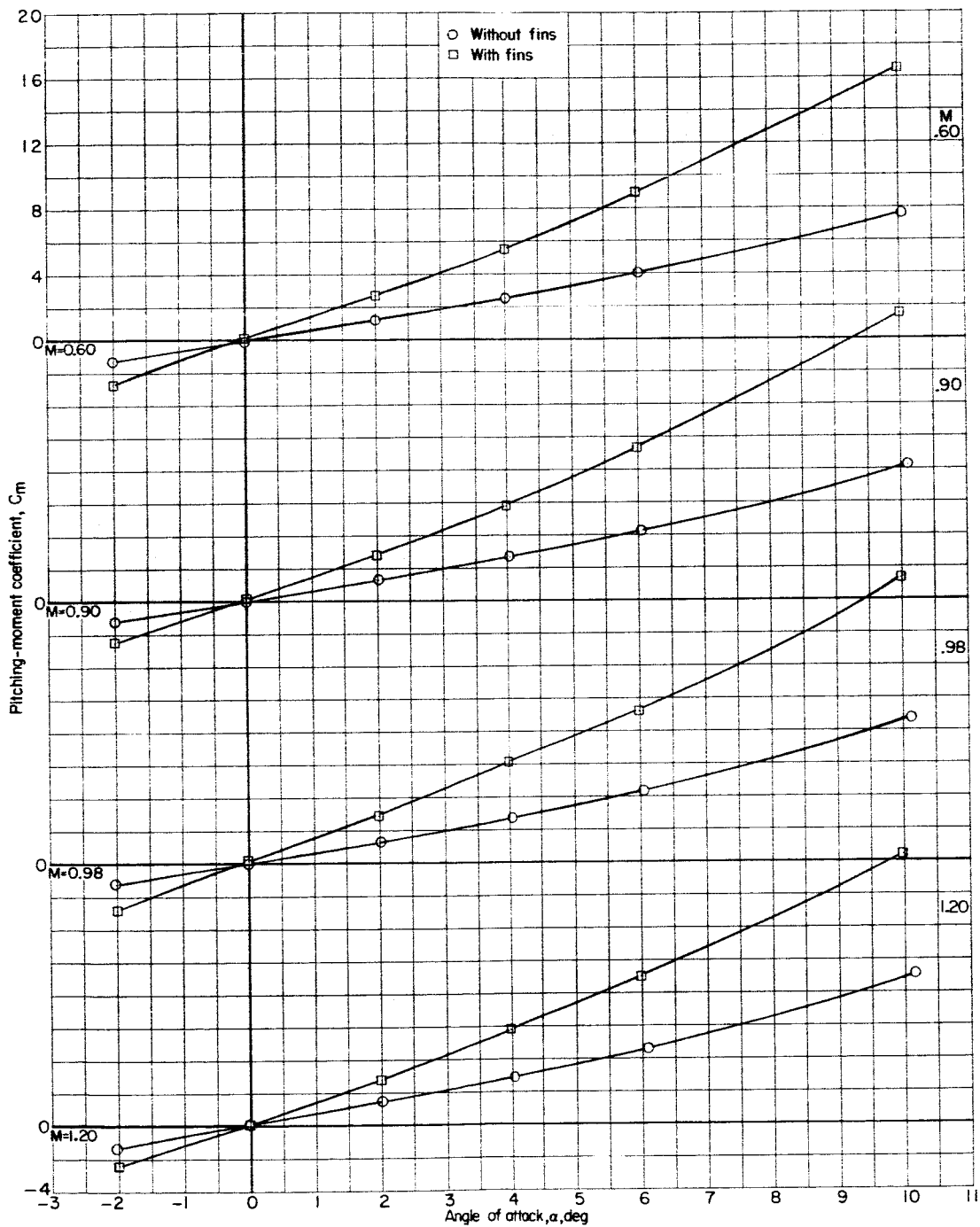
Figure 4.- Aerodynamic characteristics of the basic configuration without and with first-stage fins. $\beta = 0^\circ$.

03 10 30



(b) Axial-force coefficient against angle of attack.

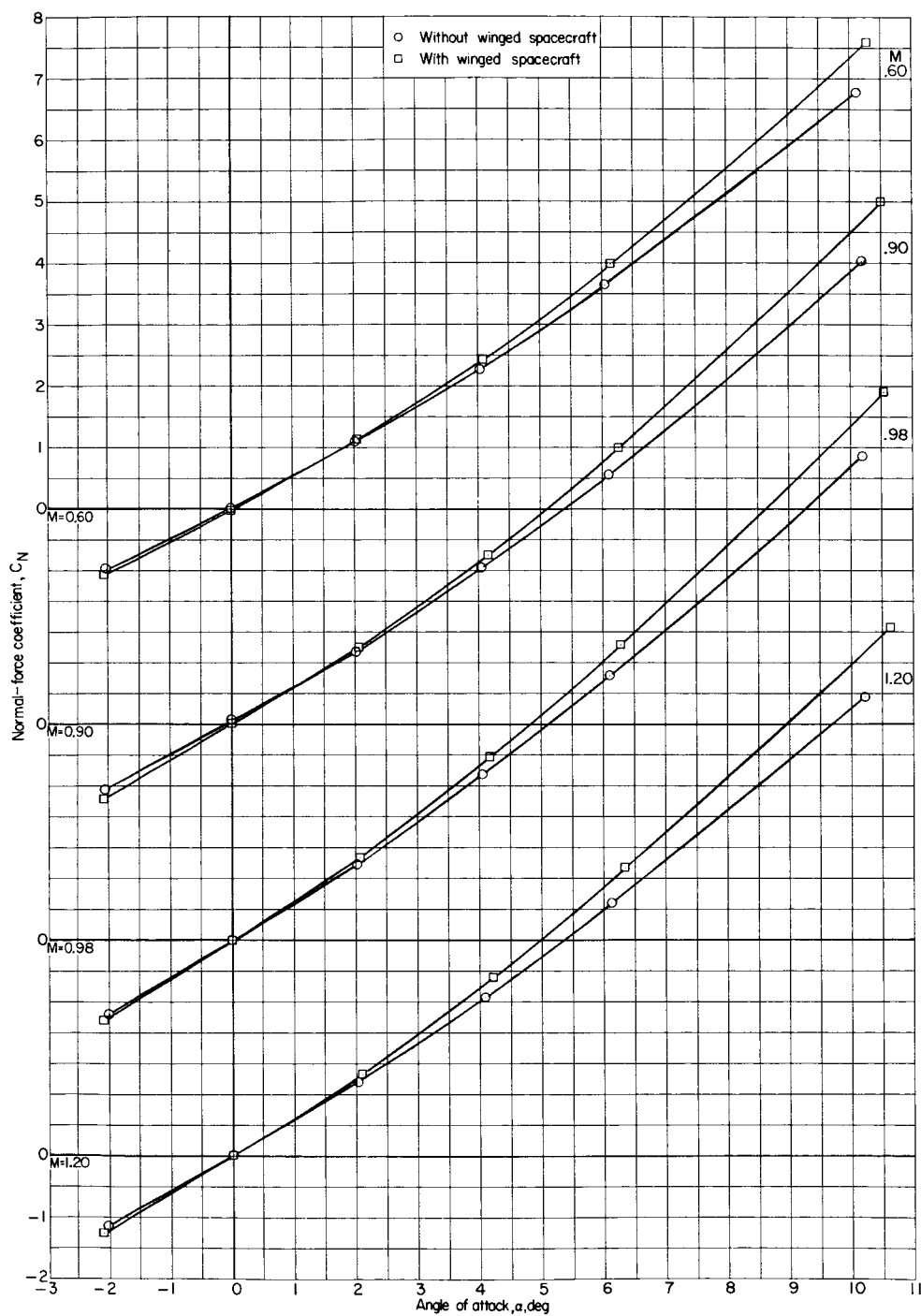
Figure 4.- Continued.



(c) Pitching-moment coefficient against angle of attack.

Figure 4.- Concluded.

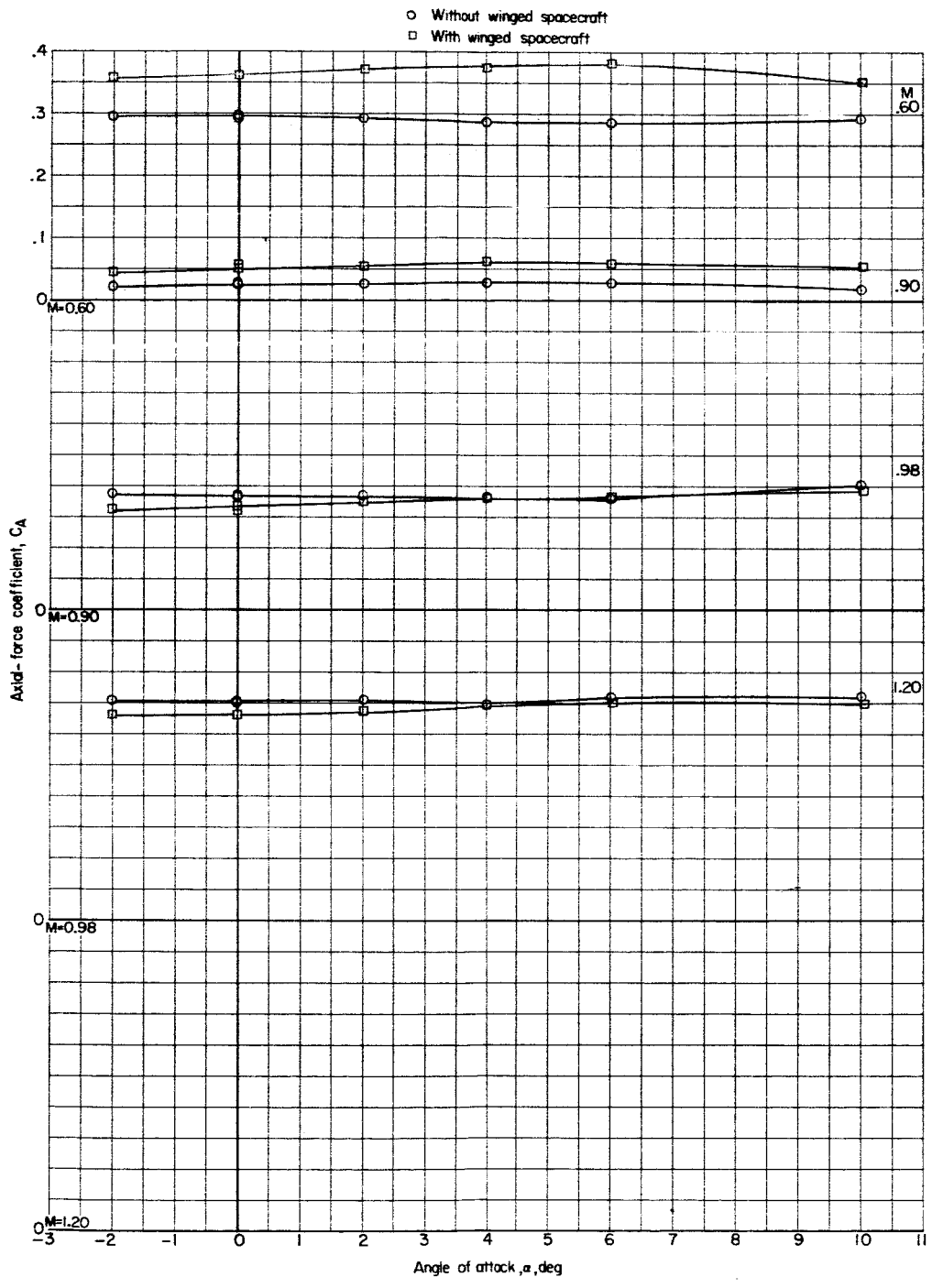
03 17 00 10 30



(a) Normal-force coefficient against angle of attack.

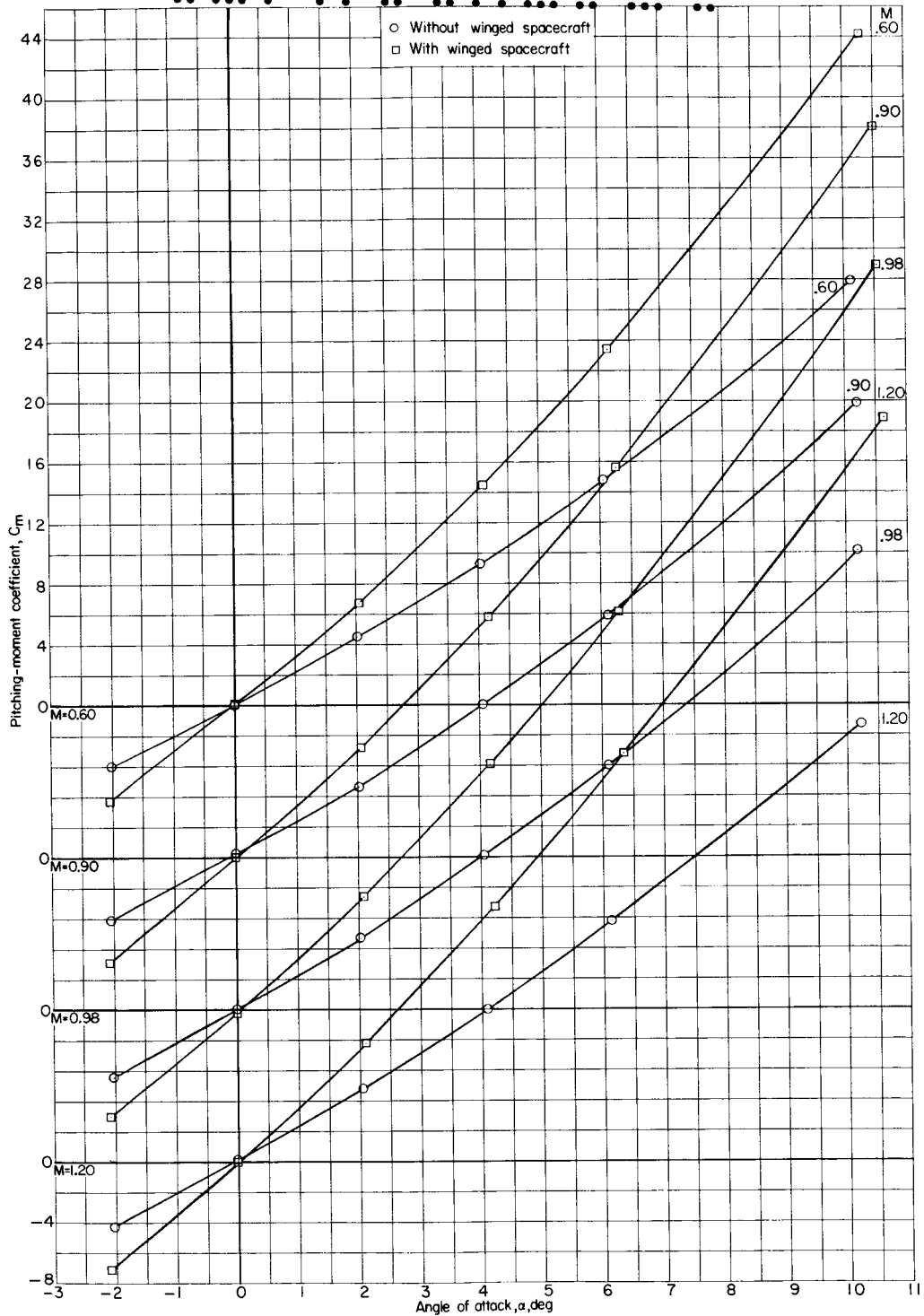
Figure 5.- Effect of the addition of second-stage fins and winged spacecraft on the aerodynamic characteristics of the finned launch vehicle. $\beta = 0^\circ$.

L-1891



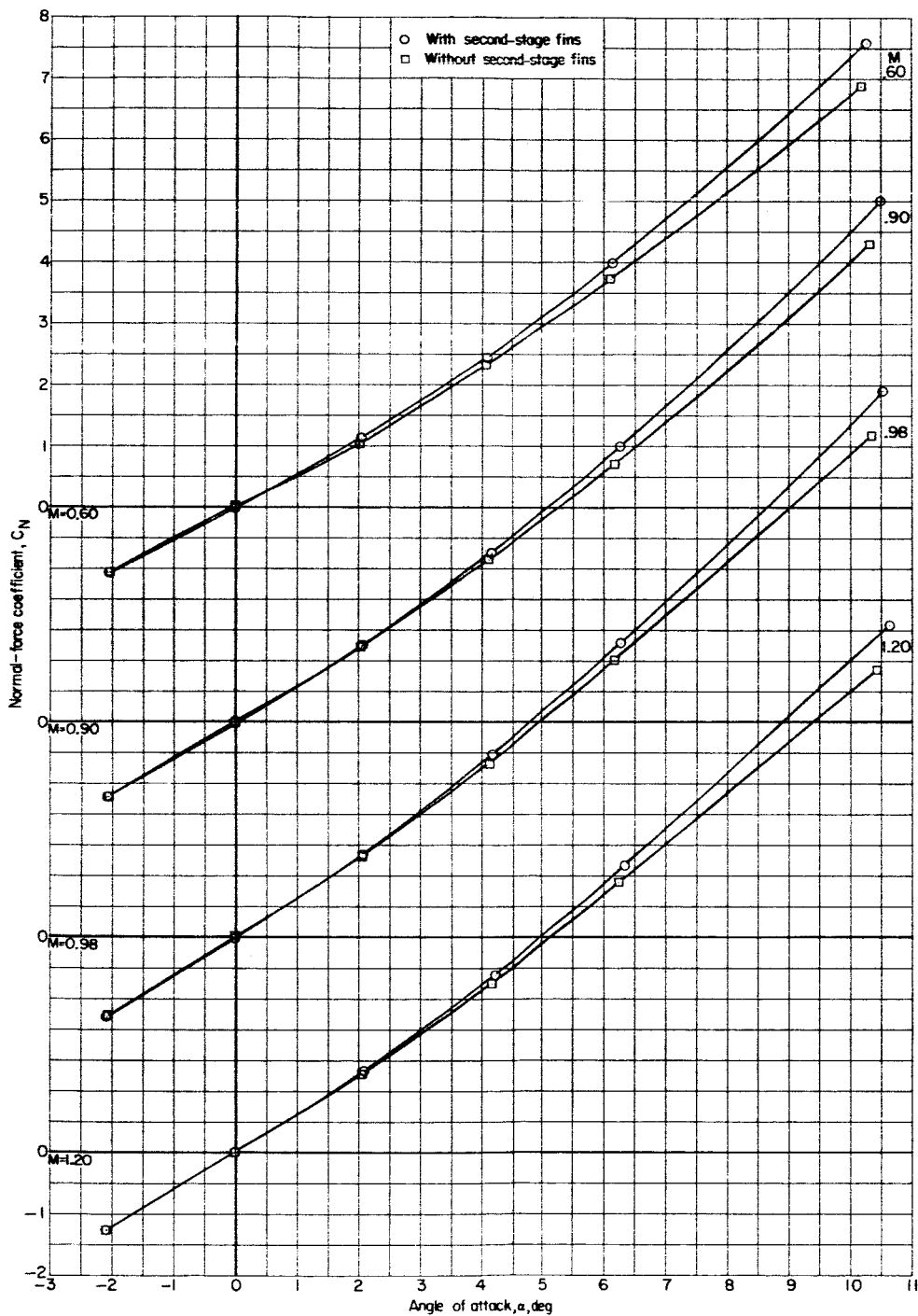
(b) Axial-force coefficient against angle of attack.

Figure 5.- Continued.



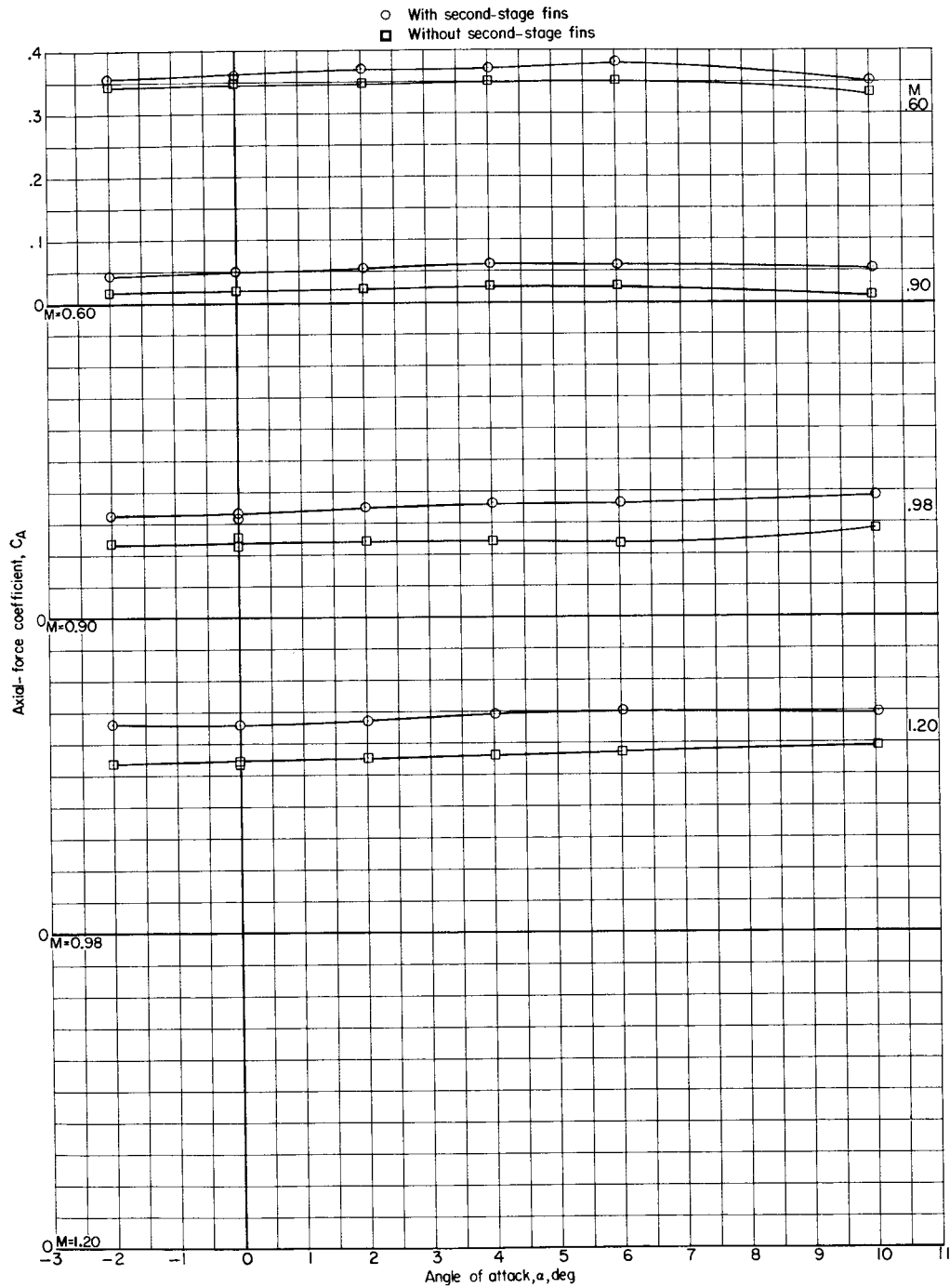
(c) Pitching-moment coefficient against angle of attack.

Figure 5.- Concluded.



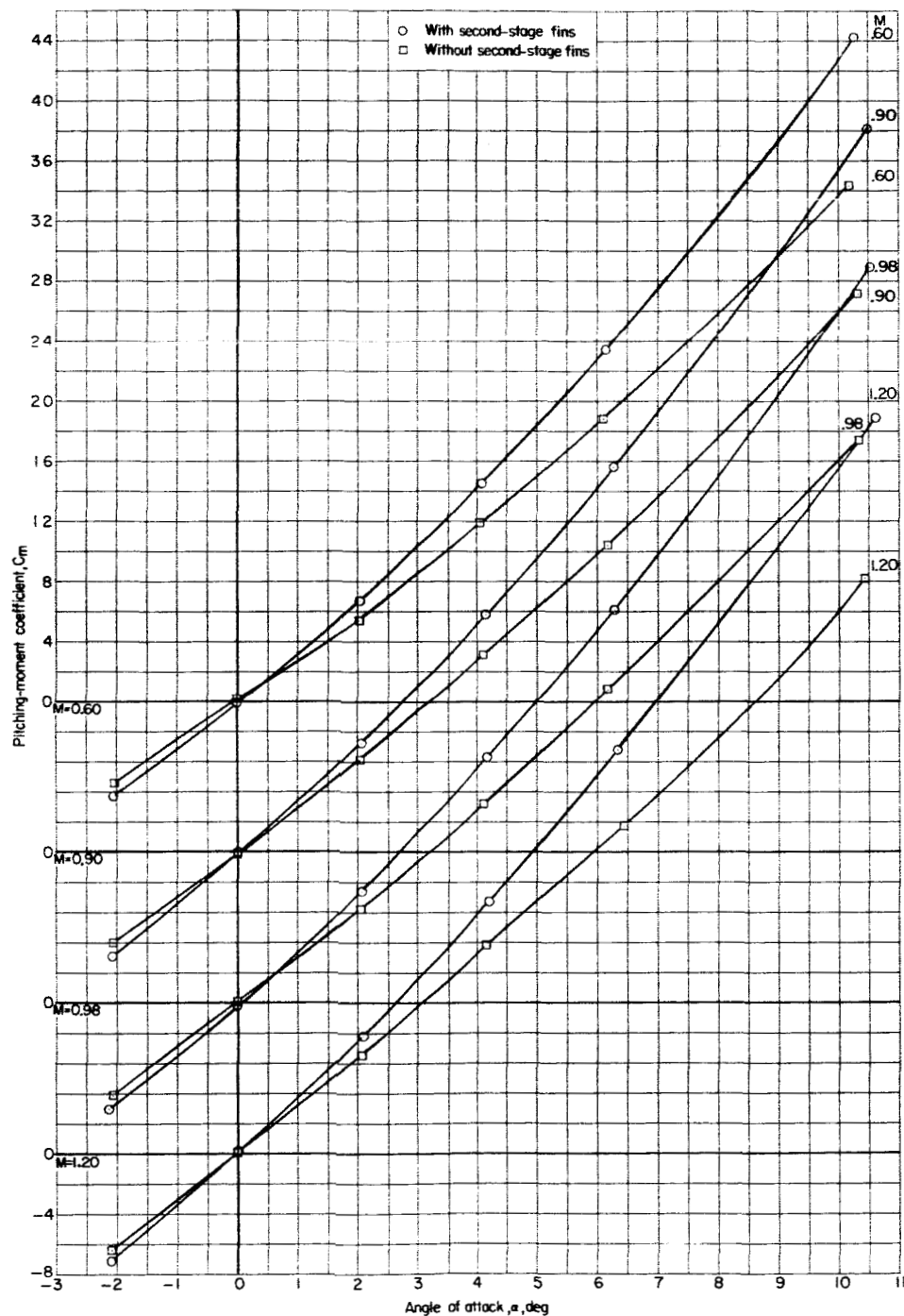
(a) Normal-force coefficient against angle of attack.

Figure 6.- Effect of removal of the second-stage fins on the aerodynamic characteristics of the model with winged spacecraft. $\beta = 0^\circ$.



(b) Axial-force coefficient against angle of attack.

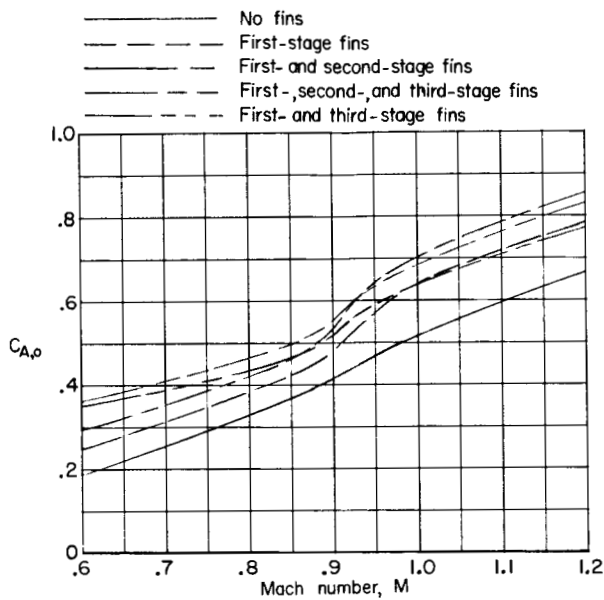
Figure 6.- Continued.



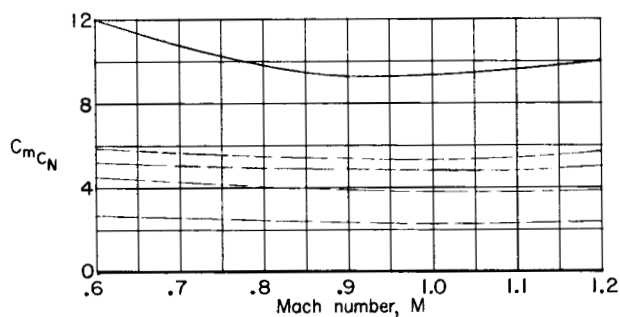
(c) Pitching-moment coefficient against angle of attack.

Figure 6.- Concluded.

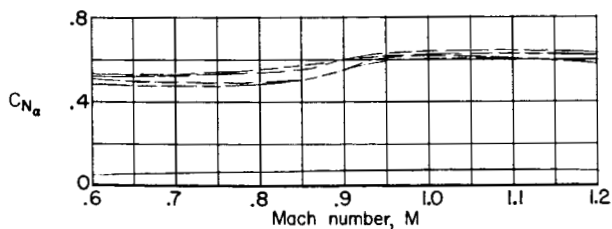
SECRET



(a) Axial-force coefficient at zero lift against Mach number.



(b) Longitudinal stability parameter against Mach number.



(c) Normal-force-curve slope against Mach number.

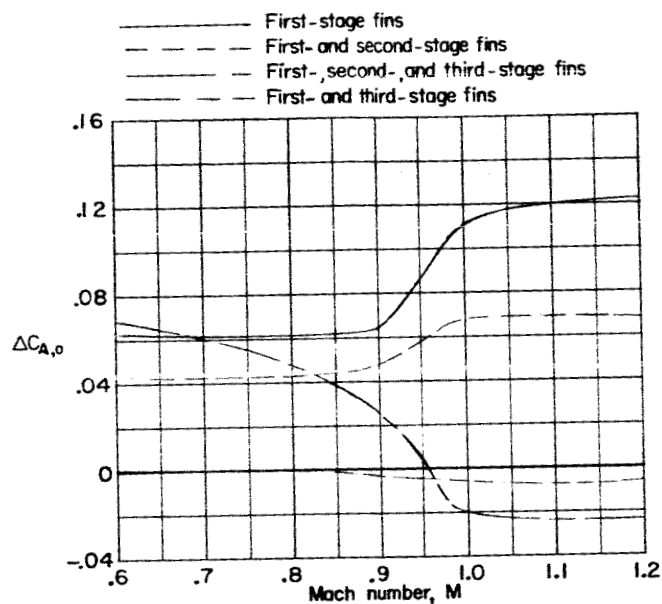
Figure 7.- Comparison of the variation with Mach number of the axial-force coefficient and longitudinal stability parameters for the several configurations. $\alpha = 0^\circ$.

SECRET

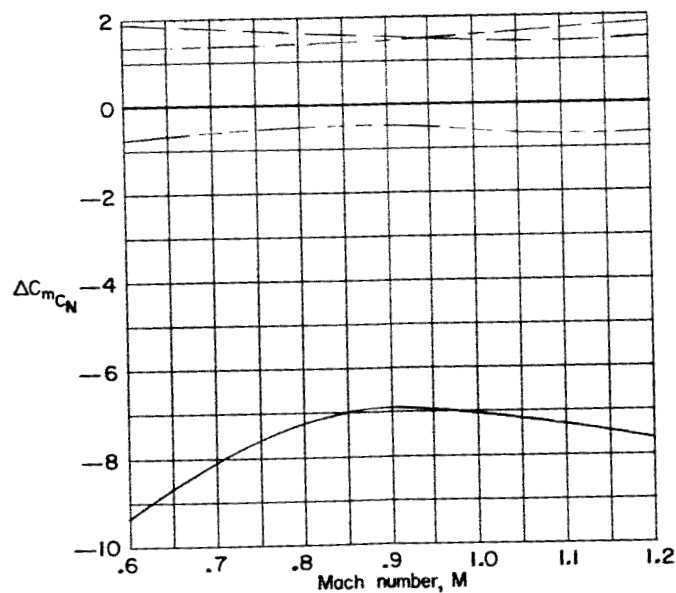
08102570
 08102570

23

I-1891



(a) Increment of axial-force coefficient at zero lift against Mach number.



(b) Increment of pitching-moment coefficient against Mach number.

Figure 8.- Interference effects of the several fin-body arrangements on the aerodynamic characteristics.

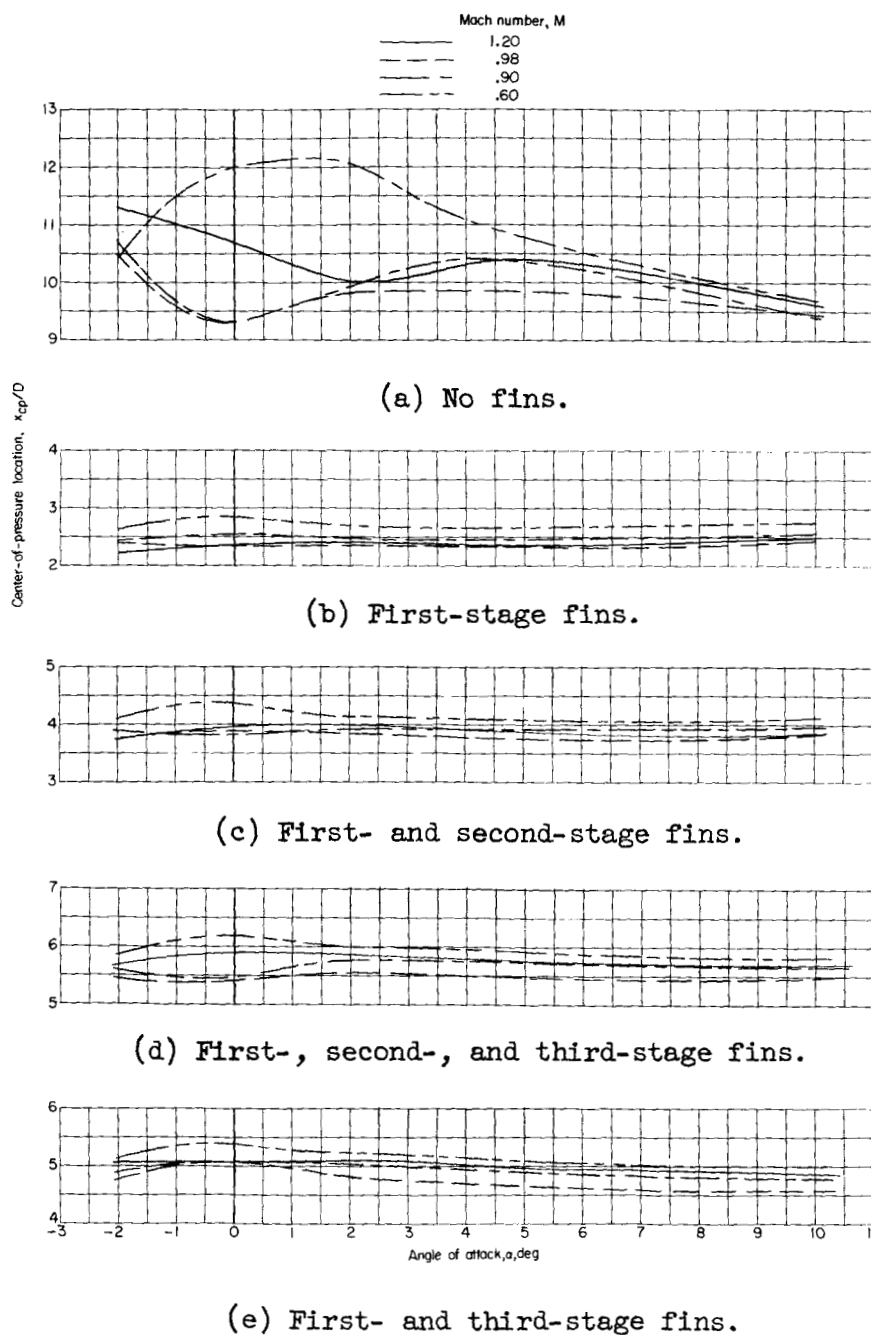
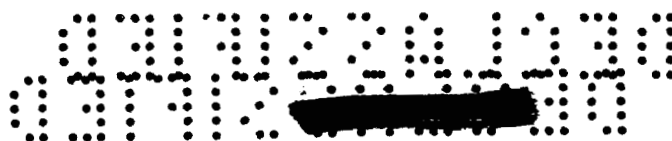


Figure 9.- Comparison of the center-of-pressure location for the several model configurations.

L-1891